

Conformal approach to cylindrical DLA

A. Taloni¹, E. Caglioti², V. Loreto³ and L. Pietronero³

¹Dipartimento di Fisica, Università di Camerino, I-62032 Camerino, Italy

²Università degli Studi di Roma “La Sapienza”, Dipartimento di Matematica P.le A. Moro 5, 00185 Rome, Italy

³Università degli Studi di Roma “La Sapienza”, Dipartimento di Fisica P.le A. Moro 5, 00185 Rome, Italy and INFM-SMC, Unità di Roma 1

E-mail: taloni@fisica.unipg.it

Abstract.

We extend the conformal mapping approach elaborated for the radial Diffusion Limited Aggregation model (DLA) to the cylindrical geometry. We introduce in particular a complex function which allows to grow a cylindrical cluster using as intermediate step a radial aggregate. The grown aggregate exhibits the same self-affine features of the original cylindrical DLA. The specific choice of the transformation allows us to study the relationship between the radial and the cylindrical geometry. In particular the cylindrical aggregate can be seen as a radial aggregate with particles of size increasing with the radius. On the other hand the radial aggregate can be seen as a cylindrical aggregate with particles of size decreasing with the height. This framework, which shifts the point of view from the geometry to the size of the particles, can open the way to more quantitative studies on the relationship between radial and cylindrical DLA.

PACS numbers: 61.43.Hv

1. Introduction

Since the Diffusion Limited Aggregation (DLA) was introduced in 1981 by Witten and Sander [1], an enormous literature has been devoted to it. Its paradigmatic role, concerning a variety of pattern formations in far-from equilibrium processes, such as DBM [2], viscous fingering [3], electrodeposition [4] etc., has made the DLA one of the most studied models by physicists in the last twenty years. Despite the simplicity of its definition, DLA gives rise to complex branching structures that cannot be described by any small perturbation of a smooth surface.

DLA was first defined on a two dimensional square lattice. Given a central particle (seed), new particles are added one by one from a far away region. The new particle performs a random walk and, when it touches the aggregate, it becomes part of it. This process is repeated as many times as the number of particles composing the cluster. One can also define the growth process in a cylindrical geometry [6]. The initial seed in this case is a base line and particles are released from a far away line parallel to the base line. Since in practice the length of the base line is finite and one uses periodic boundary conditions, topologically the growth occurs on the surface of a cylinder. We will refer to this model as “cylindrical DLA”.

The relationship between radial and cylindrical aggregates constitutes a major puzzle for the theorists since the fractal and multifractal properties of the aggregate seem definitely to depend (though in a weak way) on the geometry where the growth process occurs. Indeed, whereas the two processes (radial and cylindrical) give rise to basically similar structures, there are small but robust differences that persist to the asymptotic limit [7], and it is not obvious to conclude that they are just due to finite size effects. The value of the fractal dimension of radial DLA still represents an open and controversial question [8, 9, 10, 11, 12], whereas the most accredited one sets approximately around 1.71. On the other hand, the fractal dimension of the cylindrical DLA seems to be not so sensitive to different measurements techniques and its value, measured by box-counting method, has been approximated by 1.65 [9, 14]. Nevertheless, it is interesting to note that the value of fractal dimension measured for a circular crosscut in radial aggregates is equal to the one obtained for the intersection set of cylindrical DLA ($D_I \sim 0,65$) [15, 16, 7]. Finally, it should be stressed that recent off-lattice simulations using hierarchical maps algorithm propose an equivalence between fractal dimension of radial and cylindrical DLA [11].

The problem of the correct definition and computation of the fractal dimension is closely linked to the matter of self-similarity. For radial clusters the overall form of aggregates slowly changes during the growth, exhibiting a multi-armed shape and progressively filling the space more uniformly [17]. Indeed the structures generated by simple self-similar scaling models suggest that the lacunarity decreases with increasing size [18, 19, 17]. On the other hand cylindrical DLA does not present deviations from self-similarity, consequently his lacunarity is constant as it grows up. Roughly speaking, these discrepancies are probably due to the fact that in cylindrical DLA the cylinder size

is fixed and it does not depend on the growth process itself [9], whereas the ratio between cut-offs (size of particles and size of cluster) in radial geometry is constantly changing. In this sense the cylinder geometry offers a conceptual advantage for a theoretical discussion [9, 20], because it defines a unique growth direction and it allows to vary independently the size of the base line and the height, which are instead intrinsically linked in the radial geometry.

The two aggregates differ also on the initial *non-equilibrium* stages of their growth. Although the self affine scaling regime of the cylindrical DLA constitutes a well-known topic [13, 14, 33] lying on the surfaces' growth phenomena framework, in the radial geometry the matter of the existence of two different length scales is an open controversial question [21, 32].

Recently an elegant representation of radial DLA growth in terms of iterated conformal maps has been introduced by Hastings and Levitov [22, 23]. This formulation makes available the powerful tools of analytic function theory, leading to accurate measurements in multifractal properties of the aggregates [24, 25] and important theoretical works on the structures of these ones [27, 26].

The aim of this paper is to extend to the cylindrical geometry the analytic procedure of the conformal mapping elaborated for the radial case. The main idea behind our conformal approach is to map the unitary circle onto the interface of cylindrical cluster passing through the radial geometry. We introduce, in particular, a complex function that conformally maps the exterior of the unit circle onto the interior of an infinite stripe. Such a function allows us to shift from the radial geometry to the cylindrical one and *vice versa*. The composition of such a function with an Hastings and Levitov-like function would lead to an analytic map that transforms the exterior of the unit circle onto the complement of a cluster, growing in a stripe with periodic boundary conditions. In this way we can study the growth process of a cylindrical cluster as well as that of its radial deformation: the dimension is the same for both the aggregates as they are related by isomorphism. The same consideration also applies to the case of a “real” radial DLA that can be deformed onto a cluster growing in a periodic stripe, by composing the functions as before. In this framework the question of the relationship between the radial and the cylindrical DLA appears to be a natural and well-defined problem. In particular the cylindrical aggregate can be seen as a radial aggregate with particles of size increasing with the radius. On the other hand the radial aggregate can be seen as a cylindrical aggregate with particles of size decreasing with the height. This framework, which shifts the point of view from the geometry to the size of the particles, can open the way to more quantitative studies on the relationship between radial and cylindrical DLA.

The outline of the paper is as follows. In section II we recall the conformal mapping model for the radial DLA and we introduce the complex function that transforms the exterior of the unit circle onto an infinite periodic strip. Moreover we present the conformal mapping rules that allow to build up the cylindrical cluster. In section III we focus on the problem of the so-called unphysical particles and we discuss a new

procedure to discard them. In section IV we will deal with the question of the dimension of cylindrical DLA. We discuss the scaling behavior of the overall height of a cylindrical cluster as a function of a universal scaling variable. The self-affine and self-similar behaviours of the overall cluster's height are then carefully examined.

2. Conformal mapping approach

2.1. Radial DLA

We briefly recall the conformal mapping formulation of radial DLA [22].

Let us consider an analytic function that maps the unit circle in the mathematical w -plane onto the complement of the cluster of $n - 1$ particles in the physical z -plane. Such a function is derived from the composition of elementary maps $\varphi_{\lambda, \vartheta}$:

$$\Phi^n(w) = \Phi^{(n-1)}(\varphi_{\lambda_n, \vartheta_n}(w)). \quad (1)$$

The conformal transformation $\varphi_{\lambda, \vartheta}$ maps the exterior of the unit circle to the exterior of the unit circle with a bump of linear scale $\sqrt{\lambda}$ around the point $e^{i\vartheta}$. A choice of this function that is free of global distortion is [28]

$$\begin{aligned} \varphi_{\lambda, 0}(w) = w^{\frac{1}{2}} & \left\{ \frac{(1 + \lambda)}{2w} (1 + w) \times \right. \\ & \left. \left[1 + w + w \left(1 + \frac{1}{w^2} - \frac{2}{w} \frac{1 - \lambda}{1 + \lambda} \right)^{\frac{1}{2}} \right] - 1 \right\}^{\frac{1}{2}}, \end{aligned} \quad (2)$$

with

$$\varphi_{\lambda, \vartheta}(w) = e^{i\vartheta} \varphi_{\lambda, 0}(e^{-i\vartheta} w). \quad (3)$$

In order to obtain in the physical z -plane particles of fixed size $\sqrt{\lambda_0}$ the size of the n -th bump $\sqrt{\lambda_n}$ has to be

$$\sqrt{\lambda_n} = \frac{\sqrt{\lambda_0}}{|(\Phi^{n-1})'(e^{i\vartheta_n})|}. \quad (4)$$

We emphasize that this approximation is valid only to the first order. Fluctuation of the magnification factor $|(\Phi^{n-1})'(e^{i\vartheta_n})|$ over the unit circle on the scale of $\sqrt{\lambda_n}$, can generate particles of very unequal sizes [28] [29] (see also Section III). Furthermore it is immediate to prove that the harmonic probability on the boundary of a real cluster in z translates to an uniform measure on the unit circle:

$$P(s, ds) = d\vartheta, \quad (5)$$

where $z(s)$ is a point on the cluster's interface, and ds is an infinitesimal arc centered on this point.

In the first papers [22, 28] it was also stressed that the scaling of the cluster radius, R_n , at large n is well characterized by the scaling of the first Laurent coefficient of the mapping function (1). Indeed the Laurent expansion of Φ^n is

$$\Phi^n(w) = F_1^{(n)}w + F_0^{(n)} + \sum_{k=1}^{+\infty} F_{-k}^{(n)}w^{-k}, \quad (6)$$

so that $\Phi^n(w) \sim F_1^{(n)}w$ as $w \rightarrow \infty$. Since one expects for the radius R_n a scaling form $R_n \sim (n)^{\frac{1}{D}}\sqrt{\lambda_0}$, where D is the fractal dimension of the cluster, we can assume

$$F_1^{(n)} \sim (n)^{\frac{1}{D}}\sqrt{\lambda_0}. \quad (7)$$

The analytical form of $F_1^{(n)}$ is well-known [28]

$$F_1^{(n)} = \prod_{k=1}^n (1 + \lambda_k)^{\frac{1}{2}}. \quad (8)$$

The scaling law (7) offers a very convenient way to measure the fractal dimension of the growing cluster [28]; moreover, assuming that the total area of the cluster scales as $A_n \sim n\sqrt{\lambda_0}$ [28, 29], one can write the relation (7) as [26, 29, 30]:

$$R_n \equiv F_1^{(n)} \sim A_n^{\frac{1}{D}}. \quad (9)$$

Clearly this is true provided that individual particles areas have a sufficiently narrow distribution [29] (see Section III).

2.2. Cylindrical DLA

The essential ingredient of our conformal approach for the cylindrical DLA is the modification of the relation (4) which gives rise to a deformed radial cluster with particles of unequal sizes. That cluster will after turn into a cylindrical DLA by mean of a suitable function that shifts from the radial geometry to the cylindrical one. In this way we can adapt the conformal theory developed for the radial case to the cylindrical case, without changing the elementary function (2), as instead proposed in [11].

In the radial representation, the conformal mapping (1) can be expressed as

$$\Phi^n(w) = \Phi^{(0)} \circ \varphi_{\lambda_1, \vartheta_1} \circ \varphi_{\lambda_2, \vartheta_2} \circ \varphi_{\lambda_3, \vartheta_3} \circ \cdots \circ \varphi_{\lambda_n, \vartheta_n}(w). \quad (10)$$

As originally mentioned in [28] the choice of the initial map $\Phi^{(0)}(w)$ is flexible and one can expect the asymptotic shape of the cluster to be independent from this choice. The simplest choice of $\Phi^{(0)}(w)$ was $\Phi^{(0)}(w) = w$ [22, 28], which turns the previous definition of the mapping function in:

$$\Phi^n(w) = \varphi_{\lambda_1, \vartheta_1} \circ \varphi_{\lambda_2, \vartheta_2} \circ \varphi_{\lambda_3, \vartheta_3} \circ \cdots \circ \varphi_{\lambda_n, \vartheta_n}(w). \quad (11)$$

Let us now consider the function

$$\Xi_0^L(z) = \overline{-i \frac{L}{2\pi} \ln(z)}, \quad (12)$$

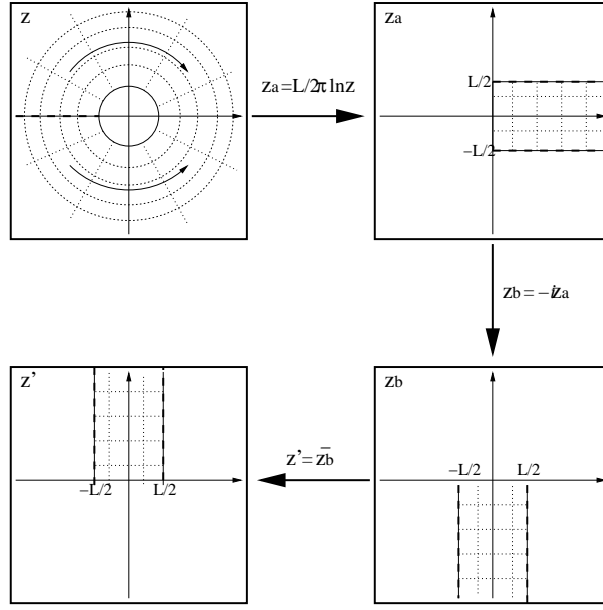


Figure 1. The action of (13) on the complex z -plane is schematically represented here. We divide the function in three steps. First box($z \rightarrow z_a$): after a cut along the negative part of the real axis (dashed line), the two parts on the half-plane $\Re e(z) < 0$ ($\Im m(z) > 0$ and $\Im m(z) < 0$) are rotated in the sense of the arrows, just as a Chinese-fan-like closure. Second box($z_a \rightarrow z_b$): the closed Chinese fan is rotated by an angle $= -\frac{\pi}{2}$. Third box($z_b \rightarrow z'$): the fan is rotated with respect the real z_b axis. The closure of the Chinese-fan is the stripe on the z' complex plane where the growth of a cylindrical aggregate occurs.

which maps the exterior of the unit circle in the z -plane, into the interior of a infinite stripe with periodic boundary conditions in the half-plane $\Im m(z') > 0$. L is a real parameter whose physical meaning is the width of the stripe in the z' -plane. A similar function was introduced for the first time in [26] with regard to the growth in a channel. If we call the polar coordinates of the z -plane ρ and θ we rewrite (12) as:

$$\Xi_0^L(z) = \begin{cases} x(\rho, \theta) &= \frac{L}{2\pi}\theta \\ y(\rho, \theta) &= \frac{L}{2\pi} \ln \rho \end{cases} \quad (13)$$

where x and y are respectively the real and the imaginary part of z' . It is possible to imagine the action of (12) on the z -plane as the closure of a Chinese fan (See Fig.1). For sake of clarity Fig.[2] shows as a square lattice on the radial plane z is deformed in the z' plane by (13).

Our choice of the function (12) seems to be the *natural link* between radial and cylindrical geometry. Indeed if we compose (12) with (11) we obtain a conformal transformation that maps the unit circle, in the w -plane, to the interface of a cylindrical aggregate in the z' -plane passing through its “radial version” in the z -plane (See Fig.3):

$$\Xi_n^L(w) = \Xi_0^L \circ \Phi^n(w). \quad (14)$$

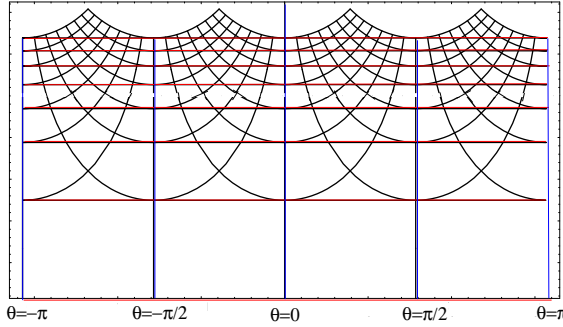


Figure 2. Deformation in z' of a square lattice in z complex plane.

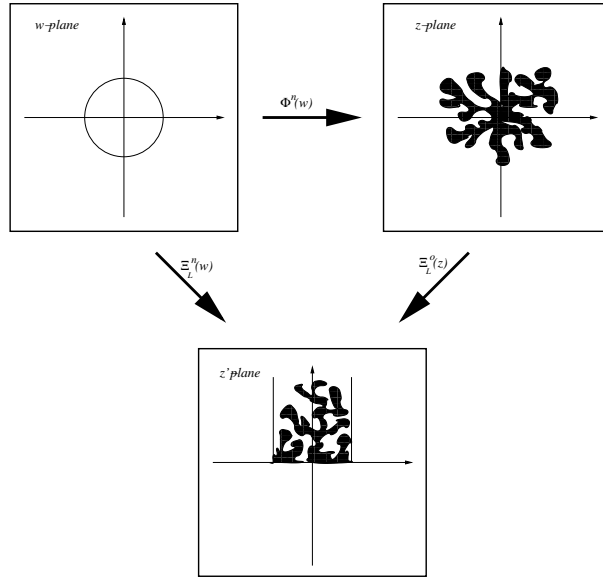


Figure 3. Sketch of the conformal approach used to construct a cylindrical aggregate. First we map the unit circle onto the interface of a radial cluster in the z -plane, by the usual Hastings and Levitov formula (1). After, we compose this function with (12). This consists in a mapping from unit circle to the cluster growing on the z' -plane.

In fact it is possible to look at the (14) as a particular form of the (10) with the $\Phi^{(0)}$ replaced by Ξ_0^L .

Let us now look, with the help of Figures [4] and [5], at the effect of the different transformations introduced. If we grow a cluster according to (1), (4), we have the “true” radial aggregate in the physical growth space (z) (Fig.4(a)). On the other hand it is possible to see this cluster deformed by (12) in the z' -plane (Fig.4(b)). Consequently in z' the size of the particles ($\sqrt{\lambda_0}$ in z) become smaller and smaller as the cluster size increases:

$$\sqrt{\lambda_n}^{(z')} = \frac{\sqrt{\lambda_0}L}{2\pi |\Phi^{(n-1)}(e^{i\vartheta_n})|} = \frac{\sqrt{\lambda_0}L}{2\pi e^{\frac{2\pi}{L}\Im m[\Xi^{(n-1)}(e^{i\vartheta_n})]}} \quad (15)$$

On the other hand if we want to construct a *real* cylindrical aggregate in z' , we have to

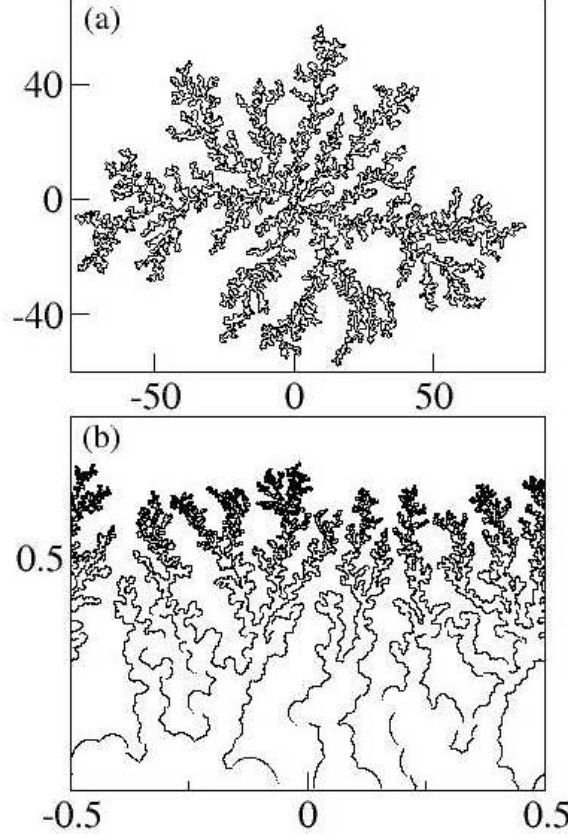


Figure 4. Radial DLA: (a) radial DLA grown with the rules (1), (4) and the acceptance criterion expressed in Section III. (b) Cylindrical deformation of the same cluster, obtained by composition of (1) with (12), note as in this plane the particle sizes decrease following (15). The simulation was performed with 10000 particles, $\lambda_0 = 0.1$ and cylinder size $L = 1$.

modify (4) in order to obtain particles of fixed size $\sqrt{\lambda_0}$ in this plane. To this end we have to divide the characteristic scale by the Jacobian of the mapping (14):

$$\begin{aligned} \sqrt{\lambda_n} &= \frac{\sqrt{\lambda_0}}{|\Xi^{(n-1)'}(e^{i\vartheta_n})|} = \frac{2\pi\sqrt{\lambda_0}|\Phi^{(n-1)}(e^{i\vartheta_n})|}{L|\Phi^{(n-1)'}(e^{i\vartheta_n})|} = \\ &= \frac{2\pi\sqrt{\lambda_0}e^{\frac{2\pi}{L}\Im m[\Xi^{(n-1)}(e^{i\vartheta_n})]}}{L|\Phi^{(n-1)'}(e^{i\vartheta_n})|}. \end{aligned} \quad (16)$$

Therefore we can grow a cylindrical cluster in the physical plane z' using (14) and (16) (Fig.5(a)) just as we grew a radial cluster in z -plane using (1) and (4). In analogy with what done for the radial case, it is possible to see the cylindrical cluster deformed by the inverse of (12) in the z -plane. In this case the size of the particles is increasing

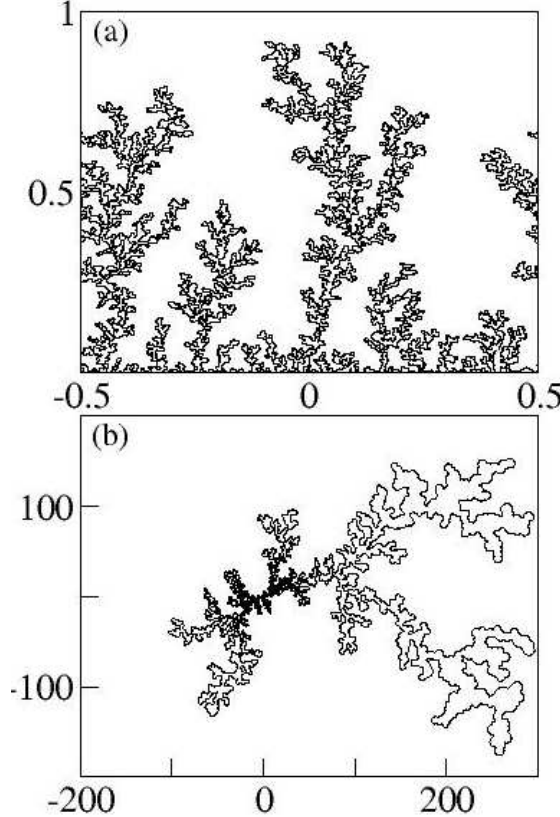


Figure 5. Cylindrical DLA: (a) cylindrical DLA grown with the rules (14), (16) and the acceptance criterion expressed in Section III. (b) Radial aggregate grown with (1), (19), conformal deformation of DLA showed in panel (a) using (12). Here $n = 10000$, $\lambda_0 = 5 \times 10^{-6}$ and $L = 1$.

exponentially with the height (y in (13)) of the aggregate (Fig.5(b)):

$$\sqrt{\lambda_n^{(z)}} = \frac{2\pi\sqrt{\lambda_0} |\Phi^{(n-1)}(e^{i\vartheta_n})|}{L} = \frac{2\pi\sqrt{\lambda_0} e^{\frac{2\pi}{L} \Im m[\Xi^{(n-1)}(e^{i\vartheta_n})]}}{L} \quad (17)$$

The complex potential on the stripe is given by

$$\Upsilon^{(n)}(\bar{z}') = \ln[(\Xi^{(n)})^{-1}(\bar{z}')], \quad (18)$$

so it is quickly verified that $P(s, ds) = d\vartheta$ on the unit circle as in radial case. Notice that the boundary conditions of the Laplacian field $\nabla P = \frac{\Phi^{(n)'}(\bar{z}')}{|\Phi^{(n)}(\bar{z}')|}$ at infinity will be automatically changed from $\nabla P \sim \frac{\hat{z}}{r}$ to $\nabla P \sim \cos \hat{\vartheta} \hat{y}$ [26].

3. Construction of the aggregate

On the original work on the radial DLA [22], it was assumed the rule (4) was sufficient to produce particles with nearly equal areas ($\sim \lambda_0$). However, as we have noticed

in the discussion after (4), this is not true in general: large particles tend to appear within fjords and seal completely large otherwise deeply invaginated regions, where the magnification factor Φ' is not constant around the bump of (3). Since our cylindrical growth model is sensitive to this problem much more than the radial one, we introduce here a fast and efficient method to eliminate too large particles.

For radial clusters, a method for the problem of abnormally stretched particles was proposed in [28] by choosing an optimal shape of bump produced by the elementary mapping $|\varphi_{\lambda,\vartheta}|$; more recently another sophisticated technique has been introduced by Stepanov and Levitov [29]. This method consists in evaluating the particle areas with unprecedented accuracy and discard the particles whose surface exceeds an acceptance threshold. Although the problem of the unphysical particles seems to be crucial in the evaluation of the cluster dimension by means of (9), for radial clusters numerical simulations suggest that the presence of large particles is irrelevant for the cluster size scaling [28, 29].

In the cylindrical case the situation is more subtle. We start by noticing that we can write (16) as:

$$\sqrt{\lambda_n} = \frac{\sqrt{\lambda_n}^{(z)}}{|\Phi^{(n-1)'}(e^{i\vartheta_n})|}. \quad (19)$$

The comparison of (19) with (4) clearly shows that it is possible to look at the aggregate grown according to (14) and (16) as a radial cluster with particles whose mean size constantly increases with the (17). Since for large n the size of the particles composing the radial version of the cylindrical DLA (see Fig.6(a)) is much larger than the one in the original radial model (i.e. $\sqrt{\lambda_n}^{(z)} \gg \sqrt{\lambda_0}$ definitely), the scale $\sqrt{\lambda_n}$ in (19) will be likely larger than the one in (4). Consequently we can expect a more important presence of filling particles than in the *simple* radial model (1), (4). An example of a typical cylindrical cluster (Fig.6(a,b)) demonstrates that there is a high number of particles that macroscopically affect the growth.

Our method to filter abnormally large particles is as follows. We recognize that every time we grow a semicircular bump with (3), we generate two new branch-cuts in the map $\Phi^{(n)}$. Each branch-cut has a pre-image on the unit circle that can be easily derived from (3):

$$w^\pm = e^{i\vartheta^\pm} = \frac{(1 - \lambda) \pm 2i\sqrt{\lambda}}{(1 + \lambda)}. \quad (20)$$

These points can be labeled by two indices [31]: $w_{j,n}$. The index j represents the generation when the branch-cut was created (i.e. when the j th particle was grown). The index n stands for the generation at which the analysis is being done (i.e. when the cluster has n particles). Indeed, after each iteration, the pre-image of each branch-cut moves on the unit circle but its physical positions does not change, so that we have a different list of “exposed” branch-cut pre-images $\{w_{j,n}\}$ each time we grow a particle.

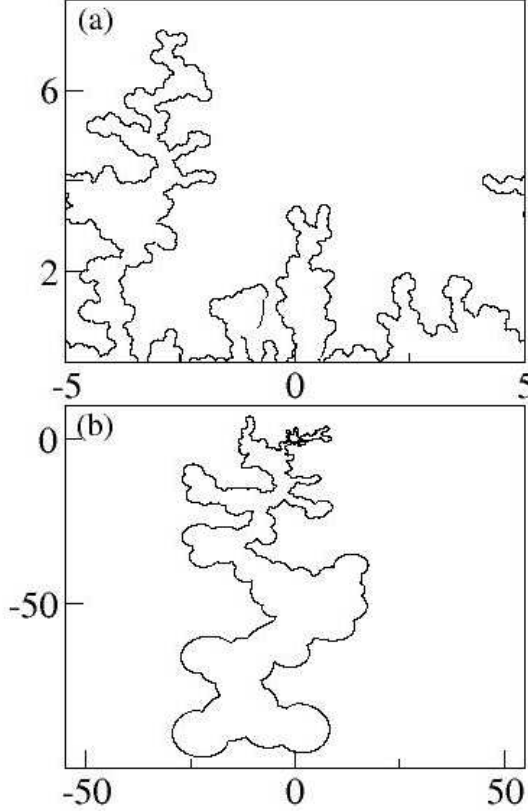


Figure 6. Cylindrical DLA: (a) cylindrical aggregate obtained by use of (14), (16) and its radial *alter ego* (b). It is possible to see how the appearance of abnormally stretched particles is frequent in this models. Other parameter simulation are: $n = 500$, $L = 10$ and $\lambda_0 = 0.011$

Indeed suppose that the list $\{w_{j,n-1}\}$ is available. In the n th generation we grow a new bump around the angle ϑ_n whose brunch-cuts are [28]:

$$e^{i\beta^\pm} = \varphi_{\lambda_n, \vartheta_n}(w_{n,n}^\pm). \quad (21)$$

If one or more of the branch-cut pre-images in the updated list $\{w_{j,n-1}\}$ is covered by the n th particle (i.e. $w_{j,n-1} \in [\beta^+, \beta^-]$ for some j), it will not be registered on the new list $\{w_{j,n}\}$, otherwise it will be included as

$$w_{j,n} = \varphi_{\lambda_n, \vartheta_n}^{-1}(w_{j,n-1}). \quad (22)$$

These values, obtained by varying j , and the sorted new pair $w_{n,n}^\pm$, will compose the n th list. The analytical form of $\varphi_{\lambda,0}^{-1}$ is [28]:

$$\varphi_{\lambda,0}^{-1} = \frac{\lambda w^2 \pm \sqrt{\lambda^2 w^4 - w^2[1 - (1 + \lambda)w^2][w^2 - (1 + \lambda)]}}{1 - (1 + \lambda)w^2} \quad (23)$$

and the inverse mapping $\varphi_{\lambda,\vartheta}^{-1}$ is given by $\varphi_{\lambda,\vartheta}^{-1}(w) = e^{i\vartheta} \varphi_{\lambda,0}^{-1}(e^{-i\vartheta} w)$. Notice that the inverse function $\varphi_{\lambda,\vartheta}^{-1}$ is analytic on the unit circle only outside the arc $[\beta^+, \beta^-]$.

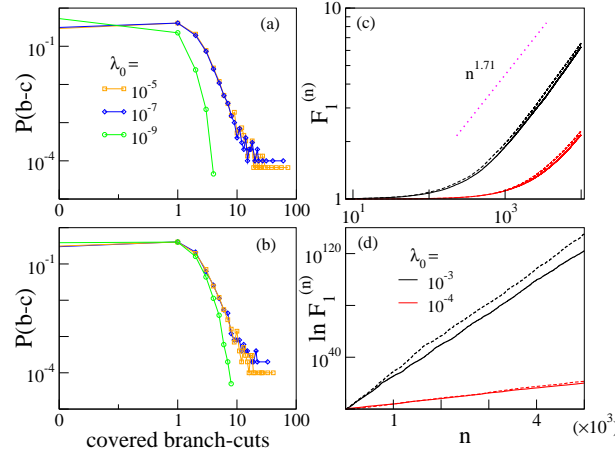


Figure 7. Controlled growth of the aggregate: (a) covered branch-cut distributions ($P(b-c)$) for radial model (1) (4), and (b) for cylindrical model (14) (16), obtained for different values of the particle size $\sqrt{\lambda_0}$; statistics was taken over 20 different realizations of the firsts 1000 growth steps setting $L = 1$. (c) scaling behavior of $F_1^{(n)}$ for radial DLA as predicted by (9) for uncontrolled growth model (solid lines) and for the proposed one (dashed lines), axes are set in logarithmic scale; the expected power-law growth of radius was drawn for reader's convenience (dotted curve). (d) Scaling behavior of the overall height of cylindrical cluster (see (24) and (25)): it is apparent as the controlled and uncontrolled growth models coincide in the limit $\frac{\sqrt{\lambda_0}}{L} \rightarrow 0$, here $L = 10$.

The branch-cut covered distributions for radial model (1) (4) and cylindrical model (14) (16) are displayed in panel (a) and (b) of Fig.7 respectively. The two distributions are equally peaked about one covered branch-cut and seem to show similar shape and the same power-law decreasing trend on the tails. Furthermore it is apparent that such tails tend to become less pronounced as the particle size decreases and to completely disappear in the limit $\sqrt{\lambda_0} \rightarrow 0, \frac{\sqrt{\lambda_0}}{L} \rightarrow 0$ (not shown).

In order to solve the problem of unphysical particles, we truncate the tails of the distributions $P(b-c)$ for both radial and cylindrical model, discarding the particles covering more than three branch-cuts. This operation is relatively fast because we know at each generation the list of the exposed branch-cut pre-images on the unit circle (see (22)). Then, for each particle added, we calculate how many branch-cuts of the previous generation the new particle covers. If this number is ≤ 3 the particle is accepted, otherwise it is discarded and a new attempt of particle growth is made.

As noticed in [29], it is not clear *a priori* whether the growth which discards too large particles is macroscopically equivalent to that without restrictions and whether such models reproduce the same lattice aggregates. However for radial and cylindrical cases the only significant proof is the comparison between the scaling exponents derived numerically and the dimensions accredited.

For this reason we plot the quantities $F_1^{(n)}$ and $\ln F_1^{(n)}$ in panel (c) and (d) of Fig.7, related respectively to the overall radius of a radial cluster (9) and to the height

of a cylindrical DLA (see (25) in Section IV). Solid lines refer to models on which any particle selection criterion is absent, whereas the dashed ones are related to the proposed controlled growth procedure. We first note as the slopes of both the curves remain unchanged by the presence or the absence of too large particles: this leads to conclude that the method of discarding particles covering more than three branch-cuts don't compromise the data extrapolation of the dimension. Moreover these are in accordance with the accredited values present in literature: 1.71 for radial DLA and 1.67 for cylindrical aggregates (see next section). However we stress that our method allows to filter out the fluctuations due to the presence of filling particle that inevitably affect the curves in panels (c) and (d) of Fig.7; such noisy behavior become more and more apparent in the cylindrical case as the ratio $\frac{\sqrt{\lambda_0}}{L}$ tends to 1.

4. Dimension, self-affinity and self-similarity

As already noticed the first Laurent coefficient scales as the radius R_n of the aggregate [22, 28] and it consequently provides an useful tool to study the scaling behavior of the cluster in the radial case. This property also applies to the cylindrical cluster in its radial deformation, so that the overall size of the cluster grown in the z -plane (Fig.5(b)) is well characterized by $F_1^{(n)}$. Moreover the radius in the z -plane is related to the height (y) in the physical plane z' by the second of (13), so that the logarithm of $F_1^{(n)}$ should represent the overall height of the cluster. Under the hypothesis that the cylindrical DLA is self-similar in squares of size $L/\sqrt{\lambda_0}$, the mean height of a cylindrical cluster composed by n particles growing in a stripe of size $L/\sqrt{\lambda_0}$ scales as:

$$y(n) \sim \frac{\sqrt{\lambda_0}^D}{L^{D-1}} n \quad (24)$$

where $\sqrt{\lambda_0}$ is the linear size of the particles. We can thus derive the scaling relation for the first Laurent coefficient in the case of a cylindrical cluster:

$$\ln F_1^{(n)} \sim 2\pi \left(\frac{\sqrt{\lambda_0}}{L} \right)^D n. \quad (25)$$

It is important to remark that the self-similar growth (24) of a cylindrical DLA is attained only in the steady state regime [14], i.e. for $n \gg \left(\frac{L}{\sqrt{\lambda_0}} \right)^D$.

Along the same lines followed in [27, 32] for radial clusters, we can argue that $\ln F_1^{(n)} \left(\frac{\sqrt{\lambda_0}}{L} \right)$ converges to a fixed point function $(\ln F_1)^*$ of the single *scaling* variable $x = \left(\frac{\sqrt{\lambda_0}}{L} \right)^D n$, attaining the linear regime (24) asymptotically ($x \gg 1$). In Fig.8 we present the average height $y(n) = \frac{L}{2\pi} \ln F_1^{(n)} \left(\frac{\sqrt{\lambda_0}}{L} \right)$ as a function of x for a typical DLA realization for $L = 1$ and $\sqrt{\lambda_0}$ ranging from 10^{-3} to 10^{-7} . Two different collapses are presented setting $D = 1.67$ and $D = 1.71$.

It is evident how all the curves reasonably collapse on to a unique scaling function

$$y(x) = Lg(x), \quad (26)$$

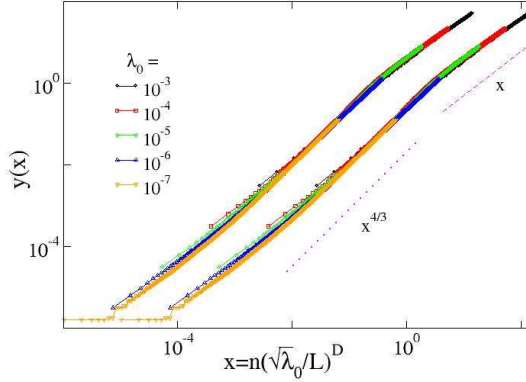


Figure 8. Overall height of a cylindrical DLA obtained for different values of the particle size $\sqrt{\lambda_0}$; the collapse on the universal scaling function (26) is apparent under the rescaling $x = n \left(\frac{\sqrt{\lambda_0}}{L} \right)^D$; the two different behaviours of $g(x)$ in (26) are also displayed for comparison: $\sim x^{1.35 \pm 0.03}$ (dotted line), and $\sim x$ (dashed line). Statistics were taken over 20 different realizations with $L = 1$. Two different collapse are displayed corresponding to $D = 1.67$ and $D = 1.71$ (shifted for clarity of one decade to the right).

with

$$g(x) \sim \begin{cases} x^{1+\beta} & y \ll 1 \\ x & y \gg 1 \end{cases} \quad (27)$$

and $\beta = 0.35 \pm 0.03$, obtained by averaging over the slopes of different curves.

Several remarks are in order:

- i) the convergence of $\ln F_1^{(n)}$ to the fixed point function is obtained infinitesimally close to the cylinder base line, for which $\ln F_1^{(n)} = 0$;
- ii) the fixed point function exists already for $x \ll 1$: in this transient regime the height of the aggregate exhibits the power-law behavior $\sim x^\alpha$, with $\alpha \simeq \frac{4}{3}$;
- iii) the predicted linear behavior is reached for $x \geq 1$.

The first two properties are also satisfied by radial clusters [32], while the third is a specific feature of cylindrical aggregates.

The property i) refers to the stage of growth before the collapse and can be roughly explained as follows.

For cylindrical self-similar clusters, if we call n_c the number of particles required to obtain one-layer coverage of the original circular interface, then $n_c \sim \left(\frac{\sqrt{\lambda_0}}{L} \right)^{(1-D)}$. Therefore $n_c \left(\frac{\sqrt{\lambda_0}}{L} \right)^D \rightarrow 0$ if $\frac{\sqrt{\lambda_0}}{L} \rightarrow 0$.

The properties ii) and iii) refer to the fixed point function: in particular ii) refers to the self-affine initial growth regime of the aggregate. The matter of self-affine growth of cylindrical DLA has been the subject of previous theoretical [33] and numerical

investigations [13, 14], both showing that the average cluster height grows as:

$$y(n) \sim L^{\frac{\nu_{\parallel}}{\nu_{\perp}}} f \left(n \left(\frac{\sqrt{\lambda_0}}{L} \right)^{\frac{1}{\nu_{\perp}}} \right), \quad (28)$$

where ν_{\parallel} is the scaling exponent of a single DLA *tree* in the transverse direction, ν_{\perp} is the scaling exponent in the growth direction and $f(x)$ is a scaling function that behaves like $\sim x^{\frac{\nu_{\parallel}}{1-\nu_{\perp}}}$ for $x \ll 1$ [34] and attains the linear regime for $x \gg 1$.

Our results indicate that the DLA dimension appears as a scaling exponent even before the self-similar regime of growth (24) sets on, thus replacing both ν_{\parallel} and ν_{\perp} in (28). Note that setting $\nu_{\parallel} = \frac{2}{3}$ and $\nu_{\perp} = \frac{1}{2}$ in accordance with [13], $g(x)$ coincides with $f(x)$ in (28).

A last remark concerns the estimate of the fractal dimension of the cylindrical aggregate, as obtained with our conformal approach. From Fig.8 it is evident how the two data collapse are not sufficiently sharp to discriminate between $D = 1.67$ and $D = 1.71$. Additional numerical work (especially for large sizes, i.e. very small values of $\sqrt{\lambda_0}$) would be necessary to check whether the asymptotic fractal dimension of the cylindrical DLA could be $D = 1.71$, as in the radial case, as suggested in [11].

5. Conclusions

In this paper we examined carefully the numerical procedure to generate the conformal maps in the cylindrical case. We have defined the conformal map as the composition of two maps: one that maps the cylindrical aggregate in a radial one, and another that map the radial aggregate in the circle. This procedure opens up new prospects on the comprehension of the relationship between the aggregates growing on different geometries. This also offers a conceptual advantage on the definition of the “right way” to calculate the fractal dimension of the DLA.

Moreover we have proposed an auto-affine scaling relation for the earlier stages of growth of the aggregate, on which the dimension of the aggregate appears as scaling exponent.

Acknowledgments

It is a pleasure to acknowledge useful discussion with Joachim Mathiessen about the numerical procedure used.

References

- [1] T.A. Witten and H.J. Sander, *Phys. Rev. Lett.* **47**, 1400 (1981).
- [2] L. Niemeyer, L. Pietronero and H.J. Wiessmann, *Phys. Rev. Lett.* **52**, 1033 (1984).
- [3] L. Paterson, *Phys. Rev. Lett.* **52**, 1621 (1984).
- [4] R.M. Brady and R.C. Ball, *Nature* **309**, 225 (1984); D. Grier, E. Ben-Jacob, R. Clarke and L.M. Sander, *Phys. Rev. Lett.* **56**, 1264 (1986).
- [5] J.W. Lyklema, C. Everstz and L. Pietronero *Europhys. Lett.* **2**, 77 (1986).

- [6] P. Meakin, *Phys. Rev. A* **27**, 2616 (1983).
- [7] B.B. Mandelbrot, A. Vespignani and H. Kaufman, *Europhys. Lett.* **32**, 199 (1995).
- [8] P. Meakin and S. Tolman in *Fractal's origin and properties*, Ed. L. Pietronero (Plenum, New York, 1989).
- [9] A. Erzan, L. Pietronero and A. Vespignani, *Rev. Mod. Phys.* **67**, 545 (1986).
- [10] B.B. Mandelbrot, B. Kol and A. Aharony, *Phys. Rev. Lett.* **88**, 055501 (2002).
- [11] R.C. Ball, N.E. Bowler, L.M. Sander and E. Somfai, *Phys. Rev. E* **66**, 026109 (2002).
- [12] For a recent paper with a good discussion of the existing literature see: A.Y. Menshutin and L.N. Schur, arXiv:cond-mat/0504338.
- [13] P. Meakin and F. Family, *Phys. Rev. A* **34**, 2558 (1986).
- [14] C. Everts, *Phys. Rev. A* **41**, 1830 (1990).
- [15] M. Kolb, *Journal de Physique* **46**, L631 (1985).
- [16] A. Arneodo, F. Argoul, E. Bacry, J.F. Muzy and M. Tabard, *Phys. Rev. Lett.* **68**, 3456 (1992).
- [17] B.B. Mandelbrot, *Physica A* **191**, 95 (1992).
- [18] P. Ossadnik, *Physica A* **176**, 454 (1991).
- [19] P. Meakin and S. Havlin, *Phys. Rev. A* **191**, 95 (1992).
- [20] M.B. Hastings, *Phys. Rev. E* **64**, 046104 (2001).
- [21] M. Plischke and Z Rácz, *Phys. Rev. Lett.* **47** 1400 (1981); M. Plischke and Z Rácz, *Phys. Rev. B* **27** 5686 (1983); P. Meakin and L.M. Sander *Phys. Rev. Lett.* **54** 2054 (1984); P. Meakin *Phys. Rev. A* **33** 3371 (1985)
- [22] M.B. Hastings and L.S. Levitov, *Physica D* **116**, 244 (1996).
- [23] M.B. Hastings, *Phys. Rev. E* **55**, 136 (1997).
- [24] M.H. Jensen, A. Levermann, J. Mathiesen and I. Procaccia, *Phys. Rev. E* **65**, 046109 (2002).
- [25] M.H. Jensen, J. Mathiesen and I. Procaccia, *Phys. Rev. E* **67**, 042402 (2002).
- [26] F. Barra, B. Davidovitch and I. Procaccia, *Phys. Rev. E* **65**, 046144 (2002).
- [27] B. Davidovitch, A. Levermann and I. Procaccia *Phys. Rev. E* **62**, R5919 (2000).
- [28] B. Davidovitch, H.G. Hentschel, Z. Olami, I. Procaccia, L.M. Sander and E. Somfai, *Phys. Rev. E* **59**, 1368 (1999).
- [29] M.G. Stepanov and L.S. Levitov, *Phys. Rev. E* **63**, 061102 (2001).
- [30] H.G. Hentschel, A. Levermann and I. Procaccia, *Phys. Rev. E* **66**, 016308 (2002).
- [31] M.H. Jensen, A. Levermann, J. Mathiesen and I. Procaccia, *Phys. Rev. E* **65**, 046109 (2002).
- [32] B. Davidovitch and I. Procaccia, *Phys. Rev. Lett.* **85**, 3608 (2000).
- [33] J.P. Nadal, B. Derrida and J. Vannimenus, *J. Phys.(Paris)* **43**, 1561 (1982).
- [34] P. Rácz and T. Vicsek, *Phys. Rev. Lett.* **51**, 2382 (1983).